Available online at www.sciencedirect.com
SCIENCE DIRECT®
Polymer 44 (2003) 4035–4045
polymer
www.elsevier.com/locate/polymer

Surface phase separations of PMMA/SAN blends investigated by atomic force microscopy

Gangyao Wen[1], Xue Li, Yonggui Liao, Lijia An*

State Key Laboratory of Polymer Physics and Chemistry, Changchun Institute of Applied Chemistry, Chinese Academy of Sciences, 159 Renmin Street, Changchun 130022, People's Republic of China

Received 9 October 2002; received in revised form 9 March 2003; accepted 17 April 2003

Abstract

The thin films of poly(methyl methacrylate) (PMMA), poly(styrene-*co*-acrylonitrile) (SAN) and their blends were prepared by means of spin-coating their corresponding solutions onto silicon wafers, followed by being annealed at different temperatures. The surface phase separations of PMMA/SAN blends were characterized by virtue of atomic force microscopy (AFM). By comparing the tapping mode AFM (TM-AFM) phase images of the pure components and their blends, surface phase separation mechanisms of the blends could be identified as the nucleation and growth mechanism or the spinodal decomposition mechanism. Therefore, the phase diagram of the PMMA/SAN system could be obtained by means of TM-AFM. Contact mode AFM was also used to study the surface morphologies of all the samples and the phase separations of the blends occurred by the spinodal decomposition mechanism could be ascertained. Moreover, X-ray photoelectron spectroscopy was used to characterize the chemical compositions on the surfaces of the samples and the miscibility principle of the PMMA/SAN system was discussed.

Keywords: Atomic force microscopy; Spinodal decomposition mechanism; PMMA/SAN blends

1. Introduction

It is well known that polymer surface plays an important role in many applications such as adhesion, protective coating, friction and wear, microelectronics, and thin film technology [1]. The surface properties of polymer blend films mainly depend on the morphologies and the phase compositions, which has motivated many fundamental studies about the phase separations of polymer blends. The phase separation phenomena in miscible polymer liquids are generally induced by variations in temperature, pressure, and composition of the blends [2]. For the liquid–liquid phase separation, the mechanism depends on the state of the thermodynamic stability of the system [3–5]. The phase diagram of a system containing simple miscibility gap can be separated into homogeneous, metastable, and unstable regions by binodal and spinodal curves. In metastable region, nucleation and growth (NG) predominate, and all small fluctuations tend to decay and hence phase separation can take place only by overcoming the barrier with a large fluctuation in composition; in unstable region, spinodal decomposition (SD) is the mechanism of phase separation, i.e. phase separation should occur by a continuous and spontaneous process without any thermodynamic barrier. The phases precipitated by the SD mechanism are interconnected with each other and have large dimensions, while those by the NG mechanism are on the contrary. Therefore, phase separation mechanisms can be judged by the analyses of the surface morphologies of the polymer blend films.

The surface morphologies of thin films can be characterized by using many methods such as scanning electron microscopy, transmission electron microscopy, and atomic force microscopy (AFM), etc. For its high surface sensitivity and simplicity of preparing samples, AFM has become a powerful technique and has been widely used to measure the surface morphology of polymer materials [1,6–17]. In addition, tapping mode AFM (TM-AFM, with high resolution and low damage to soft samples) has been

* Corresponding author. Tel.: +86-4315262206; fax: +86-4315262126.
E-mail address: ljan@ns.ciac.jl.cn (L. An).
[1] Present address: Department of Chemistry, Pohang University of Science and Technology (POSTECH), San 31, Hyojadong, Namgu, Pohang 790-784, South Korea.

0032-3861/03/$ - see front matter © 2003 Elsevier Science Ltd. All rights reserved.
doi:10.1016/S0032-3861(03)00316-1

widely employed to determine the phase morphologies of block copolymers [18–24] and polymer blends [25–30]. As a valid method, X-ray photoelectron spectroscopy (XPS) has been widely applied to studying the surface composition and the structure of polymer blends. Thermodynamic driving force for minimizing the total free energy of a system usually results in the preferential surface aggregation of the components (with a lower surface free energy) in the polymer blend and XPS has been used to characterize the surface aggregation phenomena in many polymer blends [31–37].

It has been known that poly(methyl methacrylate) (PMMA) and poly(styrene-*co*-acrylonitrile) (SAN) form a miscible blend when the acrylonitrile (AN) content in SAN is between about 9 and 33% by weight [38,39]. The phase diagrams of the PMMA/SAN systems were determined by many methods such as cloud point measurement [38], laser light scattering [39,40], and infrared microscopy [41] etc. Moreover, the miscibility principles of the PMMA/SAN blends have been debated. Because PMMA is miscible neither with polystyrene nor with polyacrylonitrile, Paul and his coworkers [38,42] suggest that the miscibility of the blends is due to the strong repulsive interactions between styrene (S) and AN segments of copolymer SAN. However, Feng et al. [43] thought that the intermolecular interactions between PMMA and SAN were responsible for the miscibility.

In this work, TM-AFM and contact mode AFM (CM-AFM) were used to study the surface phase separations of the PMMA/SAN blends annealed at different temperatures. Moreover, the chemical compositions on the surfaces of the pure components and their blends were characterized by means of XPS. On the basis of the results of XPS, the surface aggregation phenomenon and the miscibility principle of the PMMA/SAN system were discussed.

2. Experimental

2.1. Materials

PMMA ($M_w = 3.87 \times 10^5$, $M_n = 1.04 \times 10^5$, purchased from Acros) and SAN ($M_w = 1.49 \times 10^5$, $M_n = 5.6 \times 10^4$, purchased from Aldrich) with an acrylontrile (AN) content of about 30 wt% were used as received without further purification.

2.2. Sample preparation

The thin films of PMMA100 (100 represents the pure component), SAN100 and their blends were, respectively, prepared by spin-coating (3000 rpm for 30 s) their 1% (g/cm^3) 1,2-dichloroethane solutions onto silicon wafers. Prior to spin-coating, the silicon wafers were cleaned in a bath [14] of 100 ml of 80% H_2SO_4, 35 ml of H_2O_2, and 15 ml of deionized water at 80 °C for 20 min and rinsed in deionized water. The films prepared were dried under vacuum at 80 °C for 3 days and at 120 °C for 2 days to remove the residual solvent. The average thickness of the films (after being dried at 120 °C) was ca. 60 ± 5 nm evaluated with an AUEL-III type laser ellipse polarization apparatus (made in Xi'an Jiaotong University, China). The films were further annealed at different temperatures (mainly from 150 to 190 °C with 5 °C temperature step) for 30 h to form well-developed structures. According to the weight percents of SAN in the blend bulks, the blend films were, respectively, recorded as SAN20, SAN40, SAN50, SAN60, and SAN80.

2.3. AFM measurements

The surface phase morphologies of PMMA100, SAN100, and their blend films annealed at different temperatures were characterized by means of TM-AFM and CM-AFM. The AFM measurements were performed with a scanning probe microscope (SPA-300, Seiko Instruments Inc., Japan) at ambient temperature in air. In the TM-AFM and the CM-AFM measurements, the silicon cantilevers of NSC11 and CSC11 series (NT-MDT, Russia) with triangular springs were used, respectively. AFM was operated at a scan speed of 1 Hz and with a scan area of 2.0 μm × 2.0 μm. Moreover, the CM-AFM measurements were taken by scanning the tip of the cantilever in the direction orthogonal to the long cantilever axis.

2.4. XPS measurements

The surface chemical compositions of some films annealed at different temperatures were determined with a VG ESCALAB MK II spectrometer with Mg X-ray source. In this work, the pass energy of 20 eV was used to obtain the high resolution and the take-off angle of the X-ray source was 90°. The sample analysis chamber of the XPS instrument was maintained at a pressure of about 2.0×10^{-7} Pa during the spectral measurements. The chemical shift peaks are charge-referenced to the C–C/C–H peak at 284.6 eV.

3. Results and discussion

3.1. TM-AFM analyses of the pure components

The height and the phase images on the surface of a sample can be simultaneously obtained by means of TM-AFM technique. In order to compare them with those of the PMMA/SAN blends, the surface phase structures of the two pure components were investigated first. Fig. 1 shows the TM-AFM phase images of PMMA100 (left) and SAN100 (right) samples annealed at three different temperatures. It can be seen that the surfaces of PMMA100 (annealed at 120, 150, and 180 °C) and SAN100 (annealed at 120 and 150 °C)

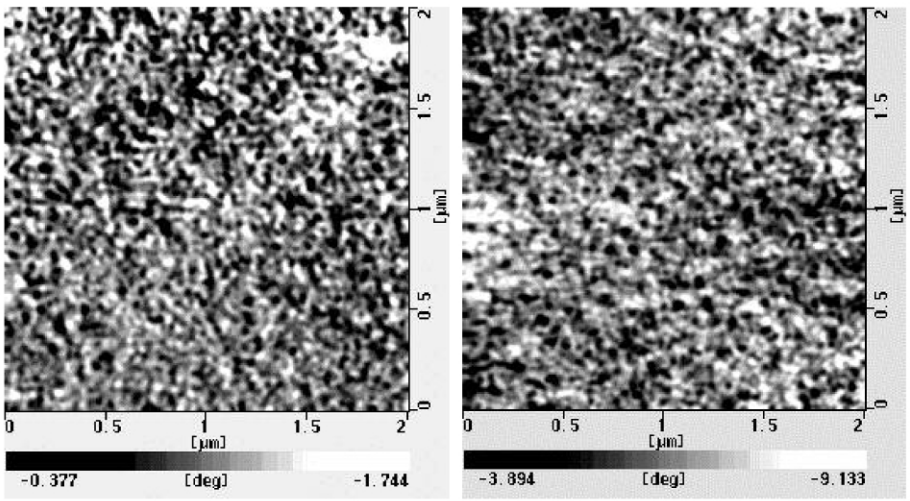

120 °C

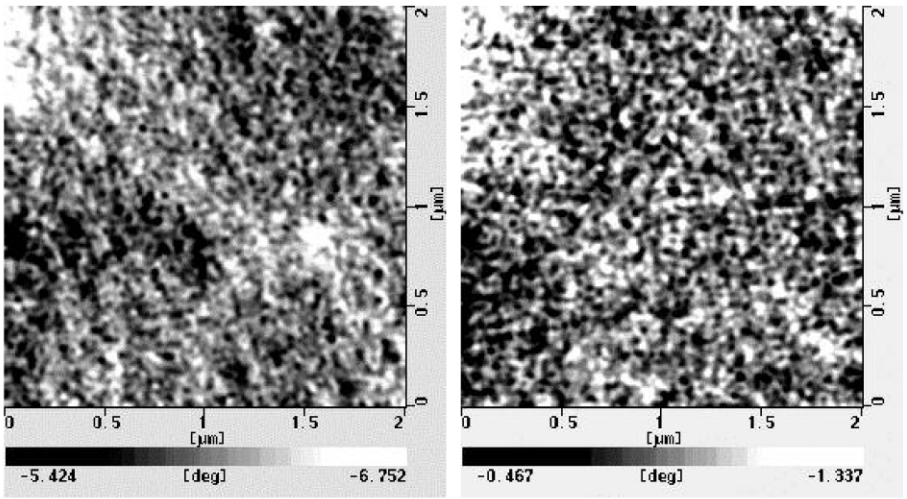

150 °C

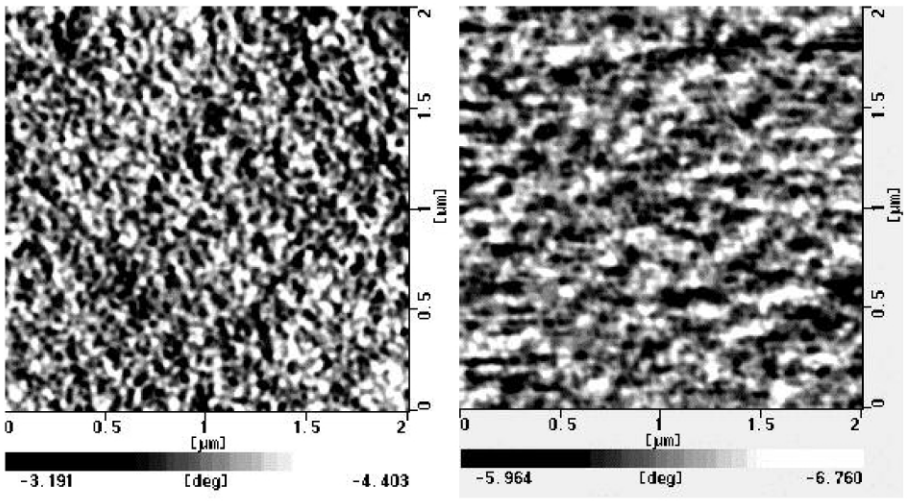

180 °C

Fig. 1. TM-AFM phase images of PMMA100 (left) and SAN100 (right) samples annealed at three different temperatures.

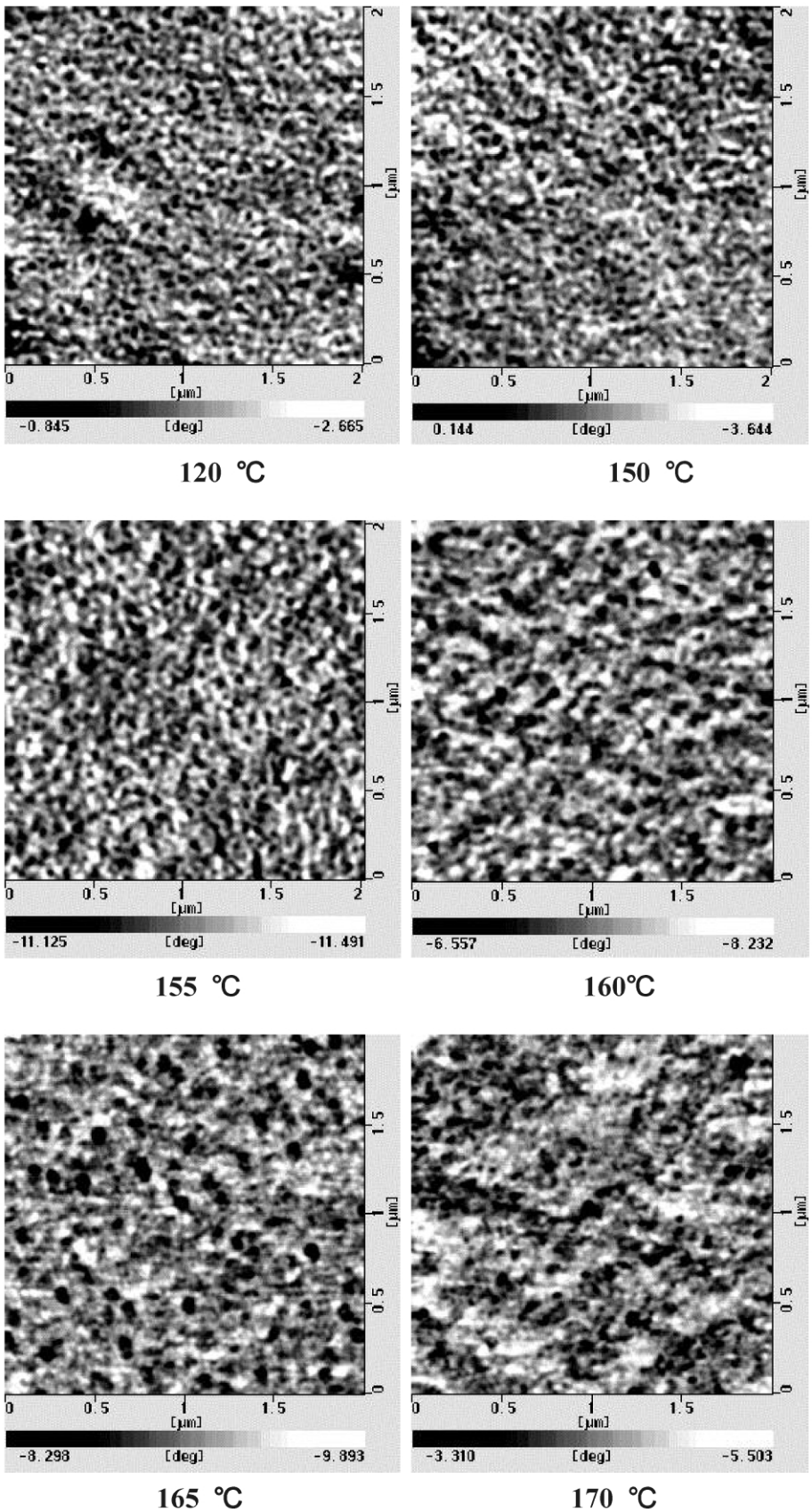

Fig. 2. TM-AFM phase images of SAN50 samples annealed at different temperatures.

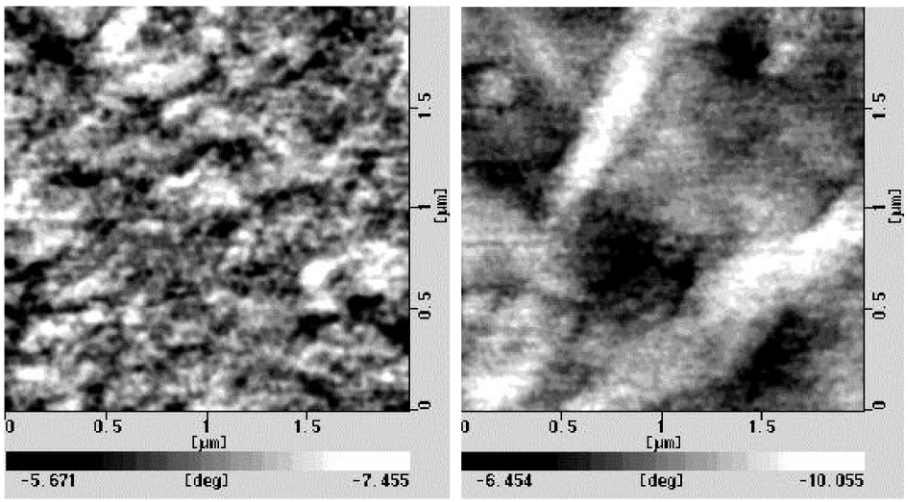

Fig. 2 (*continued*)

exhibit random morphologies and the diameters of the micro-domains are less than 50 nm. However, the surface of SAN100 annealed at 180 °C exhibits the surface enrichment phenomenon and the diameters of the micro-domains increased above 150 nm, which may be caused by the AN group strongly adsorbed to the hydrophilic substrate and the styrene (S) group tend to leave the substrate and aggregate into large micro-domains (light area).

3.2. TM-AFM analyses of the blends

All the PMMA/SAN blend samples annealed at different temperatures were also characterized by TM-AFM. As an example, the TM-AFM phase images of SAN50 samples annealed at different temperatures are shown in Fig. 2. From the TM-AFM phase images, we can find that the surfaces of the SAN50 samples annealed at 150 and 155 °C exhibit the random morphologies just like that of the sample dried at 120 °C; the surfaces of SAN50 samples annealed at 160 and 165 °C have formed the alveolate phase structures and the phase separations have occurred by the NG mechanism (with the nucleation of holes); and the surfaces of SAN50 samples annealed from 170 to 190 °C have formed large continuous phase regions (whose dimensions increase with the elevation of the annealing temperature) and the phase separations have occurred by the SD mechanism. In addition, the complete surface phase separation of sample SAN50 annealed at 190 °C has occurred and the phases have interconnected with each other without clear interfaces.

As for the other blends with different compositions, we can also judge their surface phase structures from the TM-AFM phase images. That is to say, judging from the surface morphology, we can deduce whether the phase separations have occurred on the surfaces of the blends annealed at different temperatures. Furthermore, we can identify the phase separation mechanisms according to the continuity and the dimension of the phases. From the above discussion, it can be seen that TM-AFM is suitable for studying the surface phase separations of PMMA/SAN blends.

3.3. Phase diagram of the PMMA/SAN system

Based on the TM-AFM analyses of the PMMA/SAN blends, the phase diagram of the system can be obtained. Fig. 3 shows the phase diagram of the PMMA/SAN system determined by TM-AFM. The open cycles representing the surfaces of the blends annealed at the corresponding temperatures are of the random morphologies; the solid cycles and squares represent that the phase separations have, respectively, occurred by the NG and the SD mechanisms on the surfaces of the blends; and the solid and the dashed lines represent the binodal and the spinodal curves, respectively. The lower critical solution temperature, T_c, in the phase diagram of the PMMA/SAN system is about 150 °C (the corresponding content of SAN is about 40 wt%), which is close to the experimental value (T_c = 163 °C, the corresponding content of SAN is about 35 wt%) determined by Song et al. [40] with small angle laser light scattering. According to our knowledge, the phase diagram of a blend system determined by TM-AFM has not been reported.

3.4. CM-AFM analyses of the pure components

In the following, we want to know whether CM-AFM is also suited to study the surface phase separations of the PMMA/SAN blends. The height and the friction images on the surface of a sample can be simultaneously obtained by the CM-AFM technique. The CM-AFM friction images of PMMA100 (left) and SAN100 (right) samples annealed at

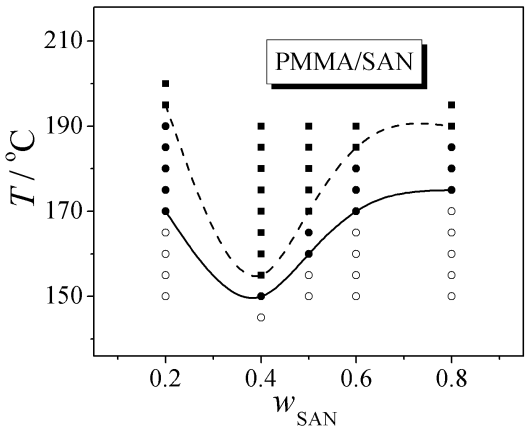

Fig. 3. Phase diagram of the PMMA/SAN system determined by TM-AFM. The open cycles represent the surfaces of the blends annealed at the corresponding temperatures are of the random morphologies; the solid cycles and squares represent the phase separations have, respectively, occurred by the NG and the SD mechanisms on the surfaces of the blends; and the solid and the dashed lines represent the binodal and the spinodal curves, respectively.

the three different temperatures are shown in Fig. 4. It is difficult for us to deduce whether phase separation has occurred on the surfaces of the sample SAN100 annealed at 180 °C. It is probably because the deformations of the soft regions resulted from the damages in the CM-AFM measurements.

3.5. CM-AFM analyses of the blends

As an example, Fig. 5 shows the CM-AFM friction images of the SAN50 samples annealed at different temperatures. From the CM-AFM friction images, it is also difficult for us to judge whether the surfaces of the SAN50 samples annealed at different temperatures are miscible or the phase separations have occurred when the annealing temperatures are lower than 170 °C. However, the surfaces of the SAN50 samples annealed from 170 to 190 °C have formed continuous phases with large dimensions (which increase with the elevation of the annealing temperature), that is, the surface phase separations have occurred by the SD mechanism, which coincides with the results determined by TM-AFM. As for the other blends, we can obtain the similar results. That is to say, CM-AFM can also be used to study the surface phase separations (by the SD mechanism) of PMMA/SAN blends.

3.6. XPS analyses

C_{1S}, O_{1S}, and N_{1S} spectra for the surfaces of PMMA100, SAN100 and their blend samples annealed at different temperatures were obtained by means of XPS. In the C_{1S} spectrum of PMMA100, there are two peaks whose binding energies are, respectively, at about 284.6 eV (the reference binding energy) and 288.4 eV. The latter peak should be attributed to the carbon in the ester group and its binding energy is a little lower than that (289.1 eV, the reference binding energy is set at 285 eV) determined by Ton-That et al. [15]. The peak positions of the other two elements are the O_{1S} peak near 532.4 eV in the PMMA spectrum and the N_{1S} peak near 399.4 eV in the SAN spectrum.

Fig. 6 shows the XPS C_{1S} spectra of PMMA100, SAN100, and their blend samples dried at 120 °C. It cannot be seen that there is any distinct chemical shift of the ester carbon peaks of PMMA100 and the blends. That is to say, there is no strong intermolecular interaction between PMMA and SAN in the miscible blends. Fig. 7 shows the XPS C_{1S} spectra of SAN50 samples annealed at different temperatures. It can be seen that the ester carbon peaks of the SAN50 samples annealed at different temperatures are at the same position, that is, the ester carbon peaks of the SAN50 samples do not have any instinct chemical shifts after the phase separations. For other blend samples, we obtained the similar results. Moreover, Naito et al. [44] did not see obvious shifts in the visual comparison of the PMMA/SAN film spectra determined by infrared spectroscopy. As for the miscibility principle for PMMA/SAN blends, therefore, we prefer the repulsive theory developed by Paul et al. [38,42].

XPS can also be used to perform quantitative analyses of the surface compositions of the blends. Ton-That et al. [15] evaluated the mole concentration of PMMA on the surfaces of PMMA/PS (polystyrene) blends by using either the elemental O/C ratio from the survey spectra or the percentage of the ester group in the C_{1S} envelopes. In this work, we evaluated the weight fractions of S and AN groups on the surfaces of SAN100 samples annealed at different temperatures by using the N/C ratio. Moreover, the weight fractions of S, AN, and methyl methacrylate (MMA) groups on the surfaces of the PMMA/SAN blends were evaluated by means of the N/C and O/C ratios.

The experimental ratio of N/C on the surface of SAN100 contains the contributions of the corresponding groups to the N_{1S} and overall C_{1S} spectra, which can be expressed as

$$\left(\frac{\mathrm{N}}{\mathrm{C}}\right)_{\mathrm{exp}} = \frac{(1-X)\mathrm{N_{AN}}}{X\mathrm{C_S} + (1-X)\mathrm{C_{AN}}} \tag{1}$$

where X and $(1-X)$ are, respectively, the molar fractions of S and AN groups on the surface; N_{AN}, C_{AN}, and C_S are, respectively, the stoichiometric atomic concentrations of nitrogen and carbon in AN and S groups ($N_{AN} = 1$, $C_{AN} = 3$, and $C_S = 8$). Therefore Eq. (1) can be rearranged as

$$X = \frac{1 - 3\left(\frac{\mathrm{N}}{\mathrm{C}}\right)_{\mathrm{exp}}}{1 + 5\left(\frac{\mathrm{N}}{\mathrm{C}}\right)_{\mathrm{exp}}} \tag{2}$$

The weight fractions of S and AN groups on the surface of SAN100 can be further evaluated by means of the following

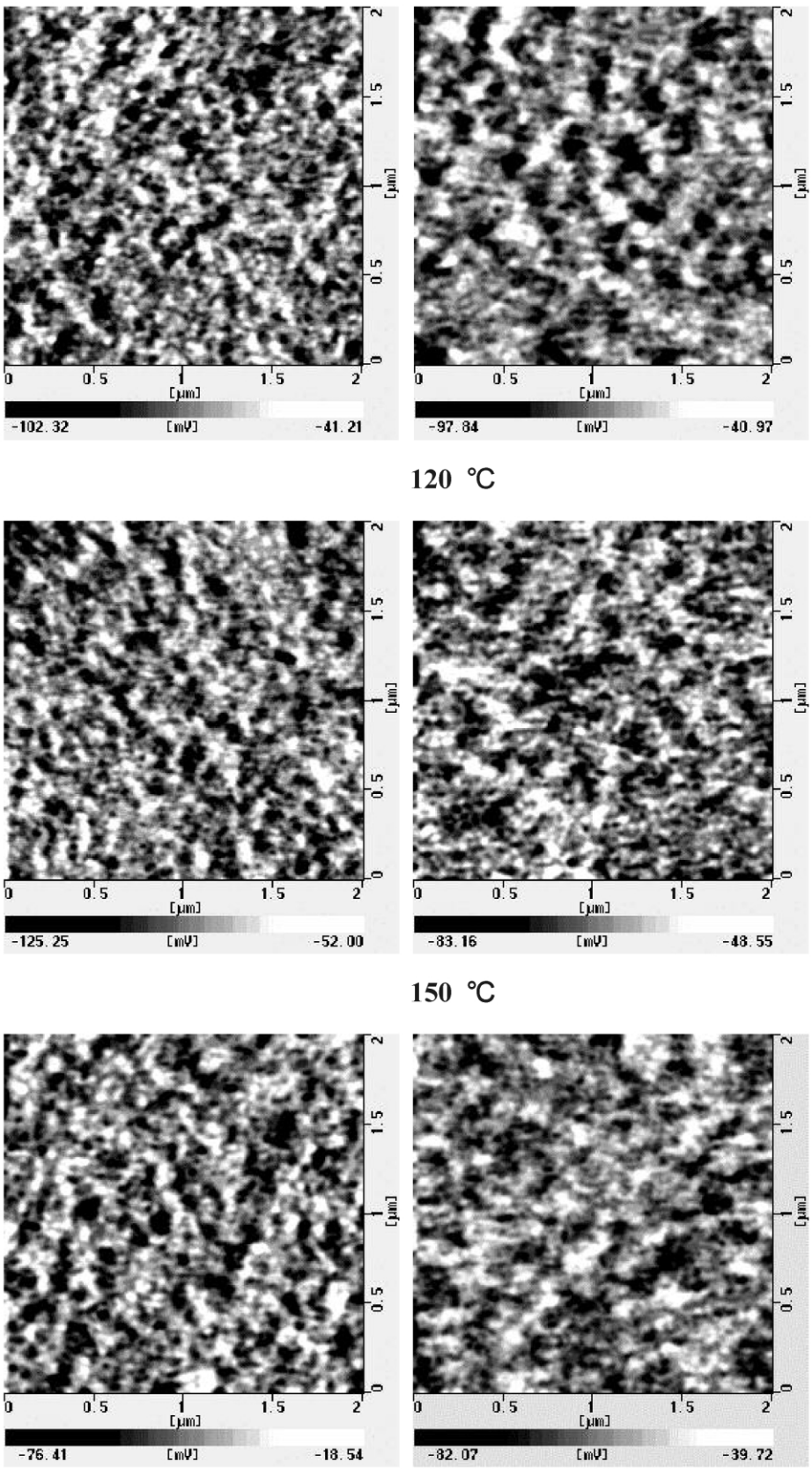

Fig. 4. CM-AFM friction images of PMMA100 (left) and SAN100 (right) samples annealed at three different temperatures.

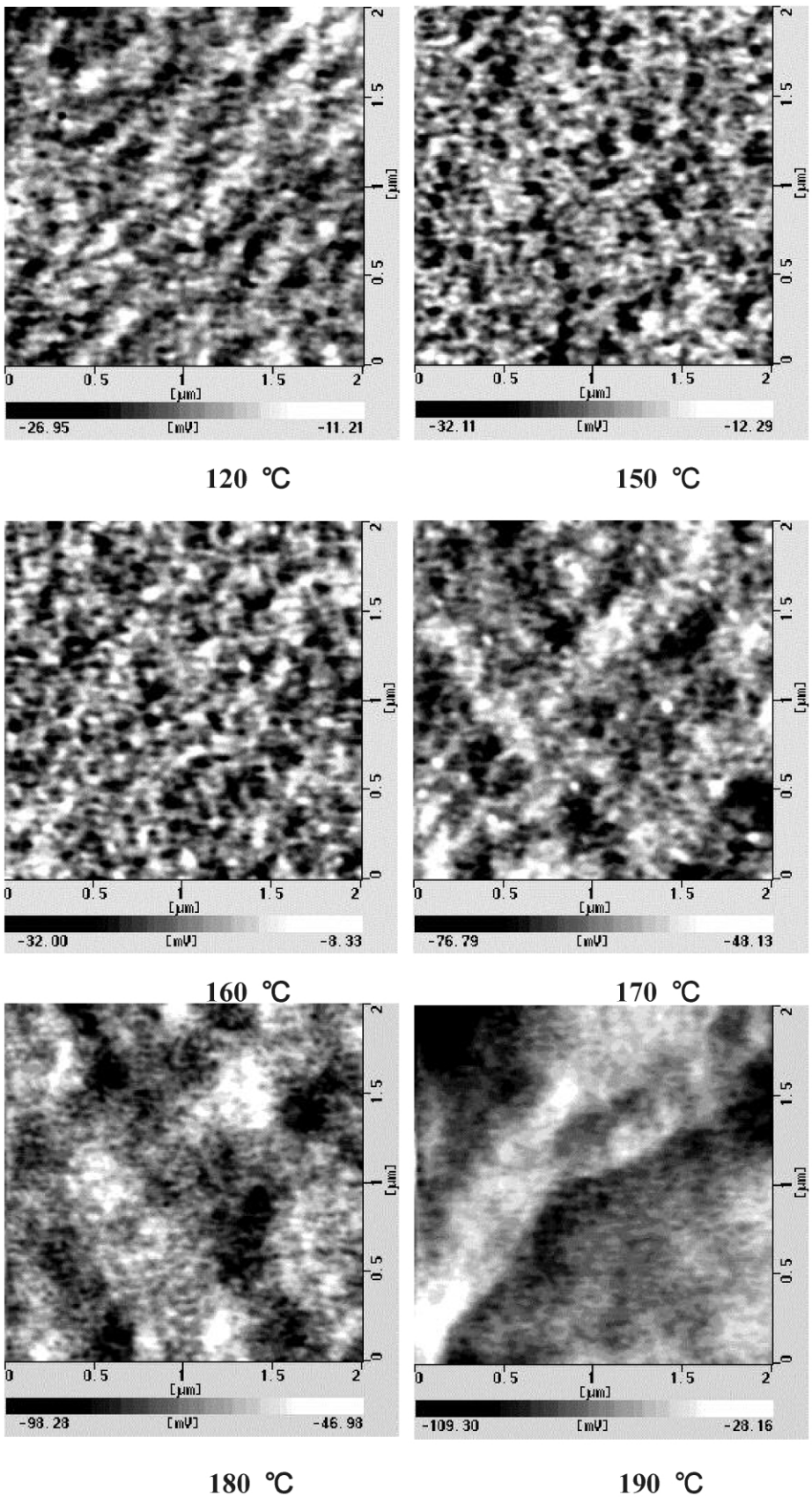

Fig. 5. CM-AFM friction images of SAN50 samples annealed at different temperatures.

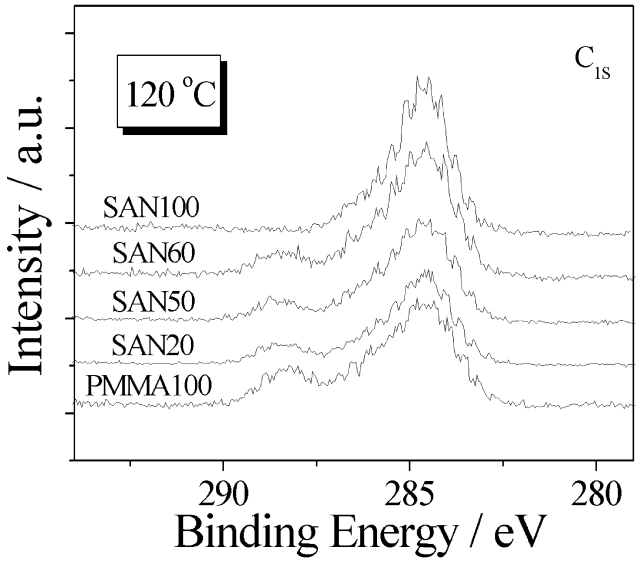

Fig. 6. XPS C_{1S} spectra of PMMA100, SAN100 and their blend samples dried at 120 °C.

equations

$$\text{wt\% (S)} = \frac{XM_S}{XM_S + (1-X)M_{AN}} \tag{3}$$

$$\text{wt\% (AN)} = 1 - \text{wt\% (S)} \tag{4}$$

where M_S and M_{AN} represent the molar masses of S and AN groups, respectively.

In the same way, the experimental ratios of N/C and O/C on the surface of the PMMA/SAN blend contain the contributions of each group to the overall N_{1S}, C_{1S}, and O_{1S} spectra, which can be, respectively, expressed as

$$\left(\frac{N}{C}\right)_{exp} = \frac{Y}{5(1-X-Y)+8X+3Y} = \frac{Y}{5+3X-2Y} \tag{5}$$

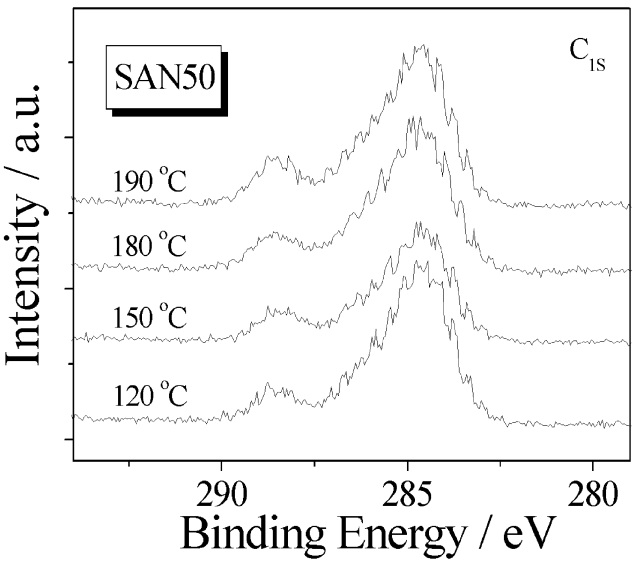

Fig. 7. XPS C_{1S} spectra of SAN50 samples annealed at different temperatures.

$$\left(\frac{O}{C}\right)_{exp} = \frac{2(1-X-Y)}{5(1-X-Y)+8X+3Y} = \frac{2-2X-2Y}{5+3X-2Y} \tag{6}$$

where X, Y, and $(1-X-Y)$ are, respectively, the molar fractions of S, AN, and MMA groups on the surface of the blend. After Eq. (5) is combined with Eq. (6), the values of X and Y can be, respectively, calculated by means of the following two expressions

$$X = \frac{2-5\left(\frac{O}{C}\right)_{exp}-6\left(\frac{N}{C}\right)_{exp}}{2+3\left(\frac{O}{C}\right)_{exp}+10\left(\frac{N}{C}\right)_{exp}} \tag{7}$$

$$Y = \frac{5\left(\frac{N}{C}\right)_{exp}+3X\left(\frac{N}{C}\right)_{exp}}{1+2\left(\frac{N}{C}\right)_{exp}} \tag{8}$$

The weight fractions of S, AN, and MMA groups on the surface of the PMMA/SAN blend can be, respectively, evaluated by virtue of the following three equations

$$\text{wt\% (S)} = \frac{XM_S}{XM_S + YM_{AN} + (1-X-Y)M_{MMA}} \tag{9}$$

$$\text{wt\% (AN)} = \frac{YM_{AN}}{XM_S + YM_{AN} + (1-X-Y)M_{MMA}} \tag{10}$$

$$\text{wt\% (MMA)} = 1 - \text{wt\% (S)} - \text{wt\% (AN)} \tag{11}$$

where M_{MMA} represents the molar mass of MMA group.

Therefore, XPS can be applied to calculating the surface weight fractions of the different groups for copolymer SAN100 and the PMMA/SAN blends annealed at different temperatures by using Eqs. (3), (4), (9)–(11), respectively. The N/C and O/C ratios and the surface weight fractions of the different groups for some samples annealed at different temperatures are listed in Table 1. It can be seen that the PMMA/SAN blends show the large surface excesses of MMA group (with the lower surface free energy) whose surface weight fractions tend to increase with the elevation of the annealing temperature except that those decrease slightly for the SAN50 and SAN60 samples annealed at 190 °C(which may be concerned with the complete phase separations of the samples). Moreover, we noticed that the nitrogen contents of the SAN20 samples (annealed at 150, 180, and 190 °C) could not be detected by XPS because the nitrogen contents on the surfaces of the samples were too low.

4. Conclusions

According to the results obtained and the above discussion, some conclusions can be drawn as follows.

(1) Comparing the TM-AFM phase images of the pure components and their blends annealed at different

Table 1
N/C and O/C ratios, and surface weight fractions of the different groups for some samples annealed at different temperatures

Sample	Annealing temperature (°C)	N/C ratio	O/C ratio	S (wt%)	AN (wt%)	MMA (wt%)
SAN100	120	0.0694	–	0.7368	0.2632	–
	150	0.0710	–	0.7311	0.2689	–
	180	0.0632	–	0.7590	0.2410	–
SAN20	120	0.0058	0.2441	0.2696	0.0170	0.7135
	150	–	0.3457	0.0886	–	0.9114
	180	–	0.3455	0.0890	–	0.9111
	190	–	0.3635	0.0585	–	0.9415
SAN50	120	0.0193	0.3212	0.0918	0.0519	0.8563
	150	0.0124	0.3081	0.1294	0.0340	0.8366
	180	0.0094	0.3670	0.0346	0.0242	0.9412
	190	0.0083	0.3510	0.0630	0.0218	0.9152
SAN60	120	0.0286	0.2326	0.2395	0.0840	0.6765
	150	0.0052	0.3669	0.0117	0.0549	0.9334
	180	0.0097	0.3805	0.0123	0.0248	0.9629
	190	0.0099	0.3381	0.0815	0.0266	0.8919
SAN80	120	0.0162	0.1040	0.5871	0.0562	0.3567
	150	0.0277	0.2466	0.2133	0.0799	0.7068
	180	0.0239	0.3240	0.0777	0.0638	0.8585
	190	0.0252	0.3494	0.0326	0.0655	0.9019

temperatures, we can deduce whether the phase separations have occurred on the surfaces of the blends. Furthermore, we can identify the phase separation mechanisms according to the continuity and the dimension of the phases. Therefore, the spinodal and the binodal curves of the PMMA/SAN system are determined by TM-AFM.

(2) Compared the CM-AFM friction images of the pure components and their blends annealed at different temperatures, the surface phase separations of the blends have occurred by the SD mechanism could be ascertained.

(3) Beginning with the N/C and O/C ratios, we have built up the expressions to calculate the surface weight fractions of the different groups for SAN100 and PMMA/SAN blends. From the analyses of the chemical compositions, it can be seen that the PMMA/SAN blends show the large surface excesses of MMA group whose surface weight fractions tend to increase with the elevation of the annealing temperature.

Acknowledgements

This work was supported by the National Natural Science Foundation of China for General (No. 20074037), Major (50290090) and Special (No. 50027001) Programs, the Special Pro-Funds for Major State Basic Research Projects (2002CCAD4000), the National Science Fund for Distinguished Young Scholars of China (No. 59825113), and the Special Funds for Major State Basic Research Projects (No. G1999064800).

References

[1] Feng J, Weng LT, Chan CM, Xhie J, Li L. Polymer 2001;42:2259.
[2] Olabisi O, Robeson LM, Shaw M. Polymer–polymer miscibility. New York: Academic Press; 1979. Chapter 2; p. 19.
[3] Gibbs W, Collected works, vol. I. New York: Longmans, Green and Co; 1928.
[4] Frenkel J. Kinetic theory of liquids. New York: Oxford University Press; 1946. Chapter VII.
[5] Cahn JW. Trans Metall Soc, AIME 1968;242:166.
[6] Binnig G, Quate CF, Gerber C. Phys Rev Lett 1986;56:930.
[7] Hansma H, Motamedi F, Smith P, Hansma P. Polymer 1992;33:647.
[8] Yang ACM, Terris BD, Kunz M. Macromolecules 1991;24:6800.
[9] Motomatsu M, Nie HY, Mizutani W, Tokumoto H. Polymer 1996;37:183.
[10] Pérez E, Lang J. Macromolecules 1999;32:1626.
[11] Saraf RF. Macromolecules 1993;26:3623.
[12] Kajiyama T, Tanaka K, Ohki I, Ge SR, Yoon JS, Takahara A. Macromolecules 1994;27:7932.
[13] Chen SA, Lee HT. Macromolecules 1995;28:2858.
[14] Buschbaum PM, O'Neil SA, Affrossman S, Stamm M. Macromolecules 1998;31:5003.
[15] Ton-That C, Shard AG, Daley R, Bradley RH. Macromolecules 2000;33:8453.
[16] Magonov SN, Elings V, Papkov VS. Polymer 1997;38:297.
[17] Zhong Q, Inniss D, Kjoller K, Elings VB. Surf Sci Lett 1993;290:L688.
[18] Dijk MAV, Berg RVD. Macromolecules 1995;28:6773.
[19] Li L, Chan CM, Li JX, Ng KM, Yeung KL, Weng LT. Macromolecules 1999;32:8240.
[20] Knoll A, Magerle R, Krausch G. Macromolecules 2001;34:4159.
[21] Stocker W, Beckmann J, Stadler R, Rabe JP. Macromolecules 1996;29:7502.

[22] Magonov SN, Cleveland J, Elings V, Denley D, Whangbo MH. Surf Sci 1997;389:201.
[23] Konrad M, Knoll A, Krausch G, Magerle R. Macromolecules 2000; 33:5518.
[24] McLean RS, Sauer BB. Macromolecules 1997;30:8314.
[25] Bar G, Thomann Y, Whangbo MH. Langmuir 1998;14:1219.
[26] Bar G, Thomann Y, Brandsch R, Cantow HJ, Whangbo MH. Langmuir 1997;13:3807.
[27] Pfau A, Janke A, Heckmann W. Surf Interf Anal 1999;27:410.
[28] Galuska AA, Poulter RR, McElrath KO. Surf Interf Anal 1997;25:418.
[29] Newby BZ, Composto RJ. Macromolecules 2000;33:3274.
[30] Kim E, Cho SJ, Suh HR, Shin DM. Thin Solid Films 1998;327–329: 42.
[31] Chiou JS, Barlow JM, Paul DR. J Polym Sci, Part B 1987;25:1459.
[32] McMaster LP. Macromolecules 1978;11:1973.
[33] Lhoest JB, Bertrand P, Weng LT, Dewez JL. Macromolecules 1995; 28:4631.
[34] Qamardeep SB, Pan DH, Koberstein JT. Macromolecules 1988;21: 2166.
[35] Goh SH, Lee SY, Dai J, Tan KL. Polymer 1996;37:5305.
[36] Kano Y, Akiyama S, Kasemura T. Int J Adhes Adhes 1997;17:207.
[37] Schmidt JJ, Gardella JJA, Salvati JL. Macromolecules 1989;22: 4489.
[38] Fower ME, Barlow JW, Paul DR. Polymer 1987;28:1177. see also p. 2145.
[39] Suess M, Kressler J, Kammer HW. Polymer 1987;28:957.
[40] Song M, Liang H, Jiang B. Chin Polym Acta 1990;2:176.
[41] Schäfer R, Zimmermann J, Kressler J, Mülhaupt R. Polymer 1997;38: 3745.
[42] Pfennig JLG, Keskkula H, Barlow JW, Paul DR. Macromolecules 1985;18:1937.
[43] Feng H, Ye C, Feng Z. Polym J 1996;28:661.
[44] Naito K, Johnson GE, Allara DL, Kwei TK. Macromolecules 1978; 11:1260.